



HAL
open science

Surface impedance of Ba_{2-x}NixAs₂ crystals

Michel Saint-Paul, Christophe Guttin, Abdellatif Abbassi, Zhao-Sheng Wang,
Huiqian Luo, Xingye Lu, Cong Ren, Hai-Hu Wen, Klaus Hasselbach

► **To cite this version:**

Michel Saint-Paul, Christophe Guttin, Abdellatif Abbassi, Zhao-Sheng Wang, Huiqian Luo, et al..
Surface impedance of Ba_{2-x}NixAs₂ crystals. Solid State Communications, 2014, 185 (1), pp.10.
10.1016/j.ssc.2014.01.014 . hal-00962469

HAL Id: hal-00962469

<https://hal.science/hal-00962469>

Submitted on 21 Mar 2014

HAL is a multi-disciplinary open access archive for the deposit and dissemination of scientific research documents, whether they are published or not. The documents may come from teaching and research institutions in France or abroad, or from public or private research centers.

L'archive ouverte pluridisciplinaire **HAL**, est destinée au dépôt et à la diffusion de documents scientifiques de niveau recherche, publiés ou non, émanant des établissements d'enseignement et de recherche français ou étrangers, des laboratoires publics ou privés.

Surface impedance of $\text{BaFe}_{2-x}\text{Ni}_x\text{As}_2$ crystals

M. Saint-Paul^{a*}, C. Guttin^a, A. Abbassi^b, Zhao-Sheng Wang^{a,c,d}, Huiqian Luo^d,
Xingye Lu^d, Cong Ren^d, Hai-Hu Wen^{d,e}, K. Hasselbach^a

^{a)}Institut Néel, CNRS et Université Joseph Fourier BP 166, F 38042 Grenoble Cedex 9 France.

^{b)}Faculté des Sciences et Techniques de Tanger, BP 416 Tanger, Université Abdelmalek Essaâdi, Morocco.

^{c)} Present address: Dresden High Magnetic Field Laboratory (HLD), Helmholtz-Zentrum Dresden-Rossendorf and TU Dresden, D-01314 Dresden, Germany.

^{d)}Institute of Physics and National Laboratory for Condensed Matter Physics, Chinese Academy of Sciences, P.O Box 603, Beijing 100190, China.

^{e)} National Laboratory for Solid State Microstructures, Department of Physics, Nanjing University, 210093 Nanjing, China.

*corresponding author E-mail address: michel.saint-paul@neel.cnrs.fr

Abstract

Measurements of the real σ_1 and imaginary σ_2 part of the conductivity were performed in optimally doped $\text{BaFe}_{1.9}\text{Ni}_{0.1}\text{As}_2$ and overdoped $\text{BaFe}_{1.88}\text{Ni}_{0.12}\text{As}_2$ crystals in the frequency range 20MHz - 1.5 GHz using a single coil technique. The temperature dependence of the London penetration depth follows a T^2 law. The conductivity σ_1 increases with decreasing temperature below T_c in agreement with the results obtained for the optimally Co doped $\text{BaFe}_{2-x}\text{Co}_x\text{As}_2$ crystals. The increase of σ_1 in the superconducting state is attributed to a rapidly decrease of the quasiparticle scattering rate.

Keywords: A. Pnictides; D. Superconductivity; E. Surface Impedance,

Introduction

A number of experimental works have been published recently concerning the surface impedance of iron based superconductors [1-6]. Low frequency, radiofrequency, microwave and optical reflectivity performed on crystals and thin films give information about the pairing of the superconducting in these materials. In particular the power law dependence of the London penetration depth in the ab plane $\lambda(T)-\lambda(0)\sim T^n$, with $n\sim 2-2.8$ [6] at $T<0.5T_c$. Such a behaviour is attributed to pair breaking scattering in the so-called s^\pm superconductivity [6]. Contradicting results on surface resistance have been reported. A coherence peak was observed in thin films with THz and optical measurements [3, 4] but no coherence peak was observed in crystals with microwave experiments [1, 2]. Here we report radiofrequency surface measurements on optimally doped $\text{BaFe}_{1.9}\text{Ni}_{0.1}\text{As}_2$ and overdoped $\text{BaFe}_{1.88}\text{Ni}_{0.12}\text{As}_2$ crystals in the frequency range 20MHz –1.5 GHz with a single coil technique. Careful analysis of the impedance measurements permits us to extract the real part of the conductivity.

Experiment

The crystal were grown using Fe/Ni-As self flux method, details are given in [7]. The samples are platelikes with the plates being perpendicular to the crystallographic c-axis, they exhibit a multicrystal structure with approximately 100 μm size single crystals which are randomly oriented in the ab plane. Samples were cleaved from a larger crystal. We selected samples with typical dimensions $1000\times 1000\times 100\ \mu\text{m}^3$, the smallest dimension is along the c axis. The platelet samples are placed inside a copper coil (11 mm length, 2.6 mm diameter, 18 turns, inductance 0.2 μHenry). The coil is situated at the end of a coaxial line inside a terminal adapter. Radio frequency magnetic field is applied parallel to the ab plane. Incident radiofrequency power was fixed to -20dBm. Non resonant measurements of the real (R) and imaginary (L) of the impedance of the coil were performed with an automated impedance analyzer Agilent 4395 in the frequency range 1-100MHz. Measurements of the self LC resonant frequency and series resistance, $L=0.2\ \mu\text{H}$, $C=50\ \text{fH}$, quality factor ~ 80 , were performed at 1.5 GHz with a Hewlett Packard 8720B network analyzer. Resistance and inductance were measured separately in the absence of a sample and were subtracted from measurements with the sample present [8].

The formulation of the impedance of the coil surrounding the sample was obtained using the equivalent circuit based on a transformer analogy developed in [9]. In this model the primary of the transformer is the measuring coil L_0 . The secondary is defined by an inductance L_2 which is related to

the eddy currents induced in the sample, L_2 is a geometrical factor and does not depend on the sample properties. The mutual inductance M between the sample and the coil is defined by the mutual inductance between the primary and secondary, $M=k^2L_0L_2$, where k is the geometrical coupling factor between the primary and secondary. The inductance of the coil is given by

$$Z = R_0 + \frac{k^2 L_0 L_2 \omega^2 R}{|R + j(X + L_2 \omega)|^2} + j \left[L_0 - \frac{k^2 L_0 L_2 \omega \{X + L_2 \omega\}}{|R + j(X + L_2 \omega)|^2} \right] \omega \quad (1)$$

Where R and X are the real and imaginary parts respectively of the surface impedance of the sample, R_0 and L_0 are the resistance and inductance of the empty coil and ω is the angular frequency.

In the experiments the same coil $L_0=0.2\mu\text{H}$ was used. Parameters $k^2\sim 0.1$ and $L_2\sim 0.6\text{ nH}$ were evaluated from the measurements in the normal state of the samples at a temperature T above superconducting transition T_c where the following equality is

$$X_N = R_N = \sqrt{\mu_0 \rho_{dc} \omega / 2} \quad (2)$$

where μ_0 is the magnetic permeability of vacuum and $\rho_{dc} = 10^6 \Omega\text{m}$ the dc sample resistivity measured in [7]. In the superconducting state R and X are deduced from equation (1).

The accuracy of our technique was tested by measurements on superconductor MgB_2 powder. Data averaging techniques were used.

Results and Discussion

The temperature dependence of R and X normalized to the value R_N measured at 25K are shown for the optimal doped $\text{BaFe}_{1.9}\text{Ni}_{0.1}\text{As}_2$ and overdoped $\text{BaFe}_{1.88}\text{Ni}_{0.12}\text{As}_2$ crystals in Figs. 1 and 2. Below T_c the frequency dependence of X/R_N observed is $\omega^{0.5}$ which is expected in the superconducting state. Reactance X is proportional to the London penetration depth and frequency [10], $X=\mu_0\omega\lambda$, in the superconducting state and $R_N\sim\omega^{0.5}$ in the normal state.

The changes in the London penetration depth $\Delta\lambda=\lambda(T)-\lambda(0)$ deduced from X/R_N are shown in Fig. 3. $\Delta\lambda$ follows a $\sim T^2$ temperature dependence at $T<T_c/2$ for optimally doped crystal.

At very low temperatures $T\ll T_c$, $\Delta\lambda$ following a power law $(T/T_c)^n$ with $n\sim 2-2.8$ attributed to the effect of strong pair breaking scattering has been reported [6].

After averaging the data, a drop of three orders of magnitude in R/R_N is obtained below the superconducting transition T_c . R/R_N is proportional to $\omega^{1.5}$, it results that the expected variation $R\sim\omega^2$ is verified in the superconducting state [10]. Nevertheless the resistance values at $T\ll T_c$ in Figs. 1 and

2 are larger by more than one order of magnitude than those reported in [1] and [2]. Similar residual surface resistance values are roughly extrapolated for the two different doped crystals in Figs.1 and 3.

Residual loss is a long standing problem in microwave studies of superconductors [11]. Residual losses are generally subtracted to obtain the intrinsic resistance. Our resistance measurements are well resolved in the vicinity of the superconducting transition. But at $T \ll T_c$ our experimental resolution is not sufficient to extract the intrinsic resistance. The real σ_1 and imaginary σ_2 part of the conductivity are related to the surface impedance Z by the following relation [10]

$$Z = R + jX = \sqrt{\frac{j\mu_0\omega}{\sigma_1 - \sigma_2}} \quad (3)$$

The real and imaginary parts of the conductivity normalized to the value $\sigma_1(25K) = \sigma_N$ at 25K in the normal state are obtained from the measurements of X/R_N and R/R_N using the following equations which are deduced from equation (3):

$$\frac{\sigma_1}{\sigma_N} = 4 \frac{RX / R_N^2}{\left[(R / R_N)^2 + (X / R_N)^2 \right]^2} \quad \frac{\sigma_2}{\sigma_N} = 2 \frac{(X / R_N)^2 - (R / R_N)^2}{\left[(R / R_N)^2 + (X / R_N)^2 \right]^2} \quad (4)$$

σ_1/σ_N and $\sigma_2/\sigma(0)$, with $\sigma_2(0) = \sigma_2(T=0)$, are shown in Figs. 4, 5 and 6.

The conductivity $\sigma_2/\sigma_2(0)$ is related to the London penetration depth [2, 10] and follows a T^2 temperature dependence:

$$\frac{\sigma_2}{\sigma_2(0)} = \frac{\lambda(0)^2}{\lambda(T)^2} \quad \text{and} \quad \frac{\sigma_2}{\sigma_2(0)} \approx 1 - \left(\frac{T}{T_c} \right)^2 \quad (5)$$

σ_1 has been calculated after elimination of the residual loss. The main effect of the subtraction of the residual loss is to force the conductivity to approach zero at zero temperature [11]. Regardless of whether or not a residual loss is subtracted, the conductivity σ_1 increases with decreasing temperature below T_c to a maximum of about 2-10 times its normal value and this maximum decreases with increasing frequency from 20 to 100MHz.

At the lowest temperatures R/R_N is small, it results that the experimental error on σ_1 is important. σ_1 depends on the subtracted residual loss and definitive conclusion about the temperature behaviour of σ_1 at the lowest temperatures remains not well known.

Our results showing an increasing of σ_1 below T_c are in agreement with the measurements on Cobalt doped $\text{BaFe}_{2-x}\text{Co}_x\text{As}_2$ crystals at 40 GHz which point out a similar behaviour [1]. The authors in [1] argue that the strong rise in the conductivity σ_1 below T_c results from a temperature dependent scattering rate decreasing rapidly with temperature.

The phenomenological two fluid model developed in [1, 10] is used here to extract the quasiparticle scattering time τ . In this two fluid model the temperature dependence of the superconducting density n_s is related to the London penetration, $n_s = \lambda(0)^2 / \lambda^2$. The normal fluid density n_n is given by $n_n = 1 - n_s$, the total carrier density being 1. It results that the temperature dependence of n_n in our experiment follows a T^2 dependence, $n_n \sim 1 - \lambda(0)^2 / \lambda(T)^2 \sim (T/T_c)^2$.

Following the two fluid model, at low frequency $\omega\tau \ll 1$, σ_1 is roughly proportional to the product $n_n\tau$ (Drude like conductivity), which gives in our case $\sigma_1 \sim n_n\tau \sim (T/T_c)^2\tau$.

Consequently scattering rate τ^{-1} is related to the normalized conductivity σ_1/σ_N by

$$\frac{\tau^{-1}}{\tau_N^{-1}} = \left[\frac{T}{T_c} \right]^2 \frac{\sigma_N}{\sigma_1} \quad (6)$$

where τ_N^{-1} is the scattering rate in the normal state at T_c .

The scattering rate deduced from σ_1/σ_N at 100MHz and 1.5GHz using equation (6) is shown in Fig6.

The temperature decrease of the scattering rate in the $\text{BaFe}_{2-x}\text{Ni}_x\text{As}_2$ can be compared with that observed in the Co doped crystals [1]. Below T_c a similar temperature decrease of τ^{-1} is observed in both Ni and Co doped BaFeAs_2 superconductors.

Conclusion

Radiofrequency measurements of real and imaginary parts of the conductivity were performed on optimally and overdoped $\text{BaFe}_{2-x}\text{Ni}_x\text{As}_2$ using a single coil technique. The temperature dependence of the London penetration depth is in agreement with the published results. The increase of the conductivity σ_1 below T_c is attributed to the temperature dependence of the quasiparticle scattering rate. A similar behaviour was observed in Co doped $\text{BaFe}_{2-x}\text{Co}_x\text{As}_2$. Strong temperature dependence of the quasi particle scattering time is observed in many unconventional superconductors [1, 11].

References

- [1] A. Barannick, N. T. Cherpak, M. A. Tanatar, S. Vitusevich, V. Skresanov, P. C. Canfield, and R. Prozorov, *Phys. Rev. B* **87** (2013) 014506.
- [2] J. S. Bobowski, J. C. Baglo, James Day, P. Dosanjh, Rinat Ofer, B. J. Ramshaw, Ruixing Liang, D. A. Bonn, W. N. Hardy, Huiqian Luo, Zhao-Sheng Wang, and Hai-Hu Wen, *Phys. Rev. B* **82** (2010) 094520.
- [3] Jie Yong, S. Lee, J. Liang, C. W. Bark, J. D. Weiss, E. E. Hellstrom, D. C. Larbalestier, C. B. Eom and T. R. Lemberger, *Phys. Rev. B* **83** (2011) 104510.
- [4] T. Fischer, A. V. Pronin, J. Wosnitza, K. Iida, F. Kurth, S. Haindl, L. Schultz, and B. Holzapfel, *Phys. Rev. B* **82** (2010) 224507.
- [5] N. Barisic, D. Wu, M. Dressel, L. J. Li, G. H. Cao, and Z. A. Xu, *Phys. Rev. B* **82** (2010) 054518,
- [6] R. Prozorov and V. G. Kogan, *Rep. Prog. Phys.* **74** (2011) 1245051-12450520.
- [7] Yanchao Chen, Xingye Lu, Meng Wang, Huiqian Luo and Shiliang Li, *Superconducting. Sci. Technol.* **24** (2011) 065004-065008.
- [8] A. Gauzzi, J. Le Coche, G. Lamura, B. J. Jönsson, V. Gasparov, F. R. Ladan, B. Plaçais, P. A. Probst, D. Pavuna, and J. Bok, *Rev. Sci. Instrum.* **71**, (2000), 2147-2153.
- [9] Yann Le Bihan *NDT&E International* **36** (2003) 297-302.
- [10] M. R. Trunin and A. A. Golubov

Spectroscopy of High Tc superconductors, Editor N. M. Plakida, Taylor & Francis Ltd (Eds), London, United Kingdom (2003) 159-233.

[11] D. A. Bonn, Ruixing Liang, T. M. Riseman, D. J. Baar, D. C. Morgan, Kuan Zhang, P. Dosanjh, T. L. Duty, A. MacFarlane, G. D. Morris, J. H. Brewer, W. N. Hardy, C. Kallin, and A. J. Berlinsky,

Phys. Rev. B **47** (1993) 11314.

Figure Captions

Figure 1

Temperature dependence of X/R_N (filled symbols) and R/R_N (open symbols) of surface impedance normalized to the value R_N obtained at 25 K for the optimally doped $\text{BaFe}_{1.9}\text{Ni}_{0.1}\text{As}_2$ crystals. Inset: Frequency dependences of X/R_N and R/R_N at 10K

Figure 2

Temperature dependence of X/R_N (filled symbols) and R/R_N (open symbols) of surface impedance normalized to the value R_N obtained at 25 K for the overdoped $\text{BaFe}_{1.88}\text{Ni}_{0.12}\text{As}_2$ crystals.

Inset: Frequency dependences of X/R_N and R/R_N at 10K.

Figure 3

Temperature dependence of the London penetration depth variation $\Delta\lambda = \lambda - \lambda(0)$ at different frequencies.

Figure 4

Temperature dependence of the real σ_1/σ_N (filled symbols) and imaginary $\sigma_2/\sigma_2(0)$ (open symbols) parts of the conductivity normalized to the value σ_N at 25 K for the optimally doped $\text{BaFe}_{1.9}\text{Ni}_{0.1}\text{As}_2$ crystals. Solid line is calculated with $1-(T/20)^2$.

Figure 5

Temperature dependence of the real σ_1/σ_N (filled symbols) and imaginary $\sigma_2/\sigma_2(0)$ (open symbols) parts of the conductivity normalized to the value σ_N at 25 K for the over doped $\text{BaFe}_{1.88}\text{Ni}_{0.12}\text{As}_2$ crystals. Solid line is calculated with $1-(T/16)^2$.

Figure 6

The temperature dependence of the quasiparticle scattering rate deduced from the conductivity $\sigma_{\square}/\sigma_N$ with Eq. 6.

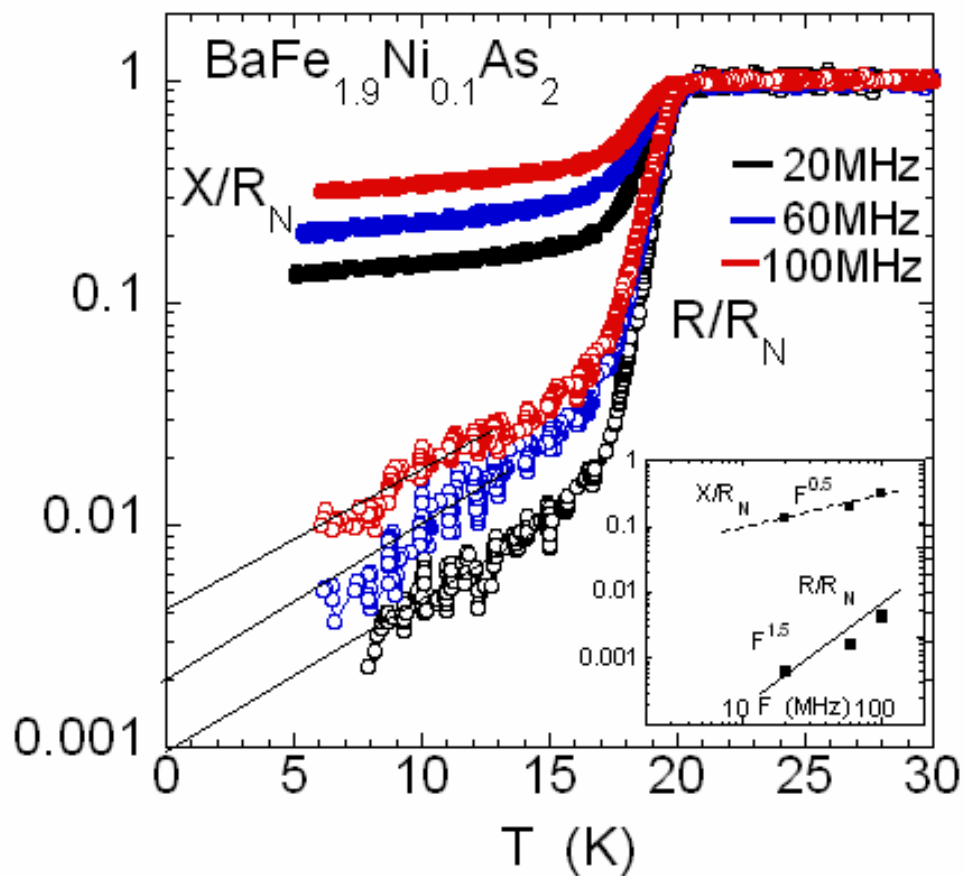


Fig1

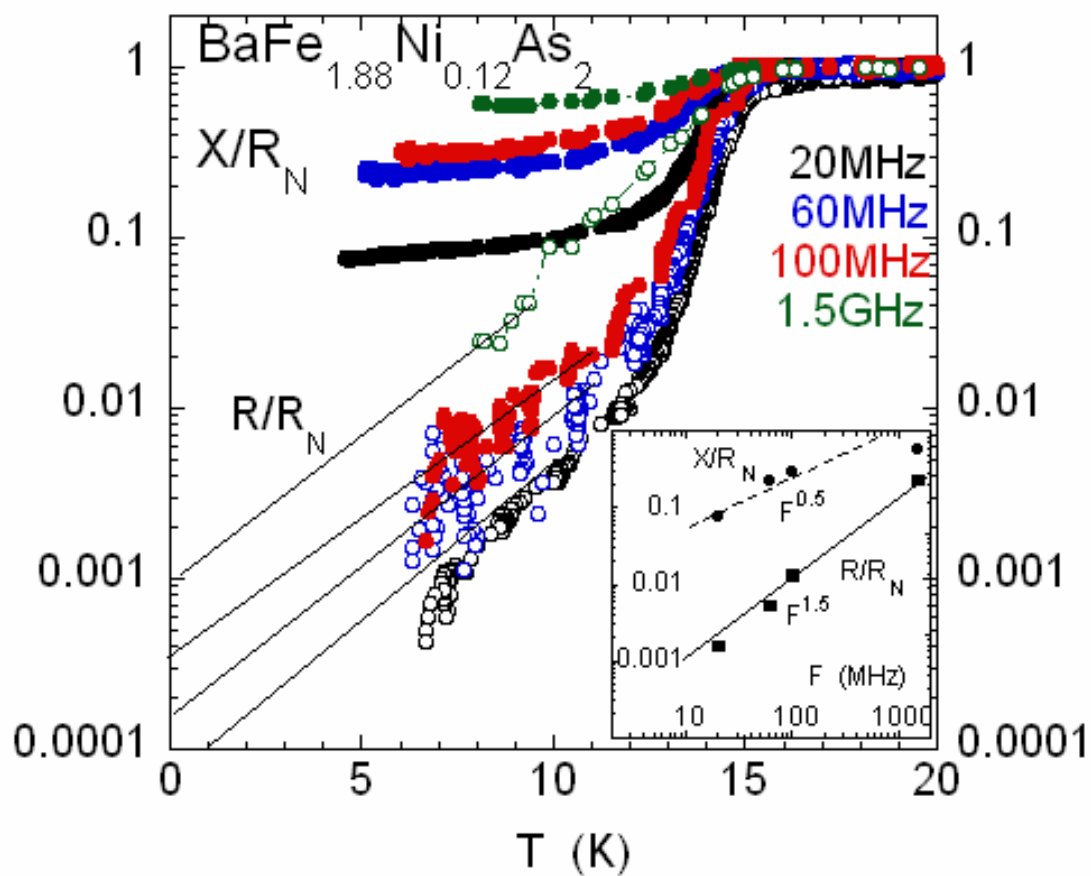


Fig2

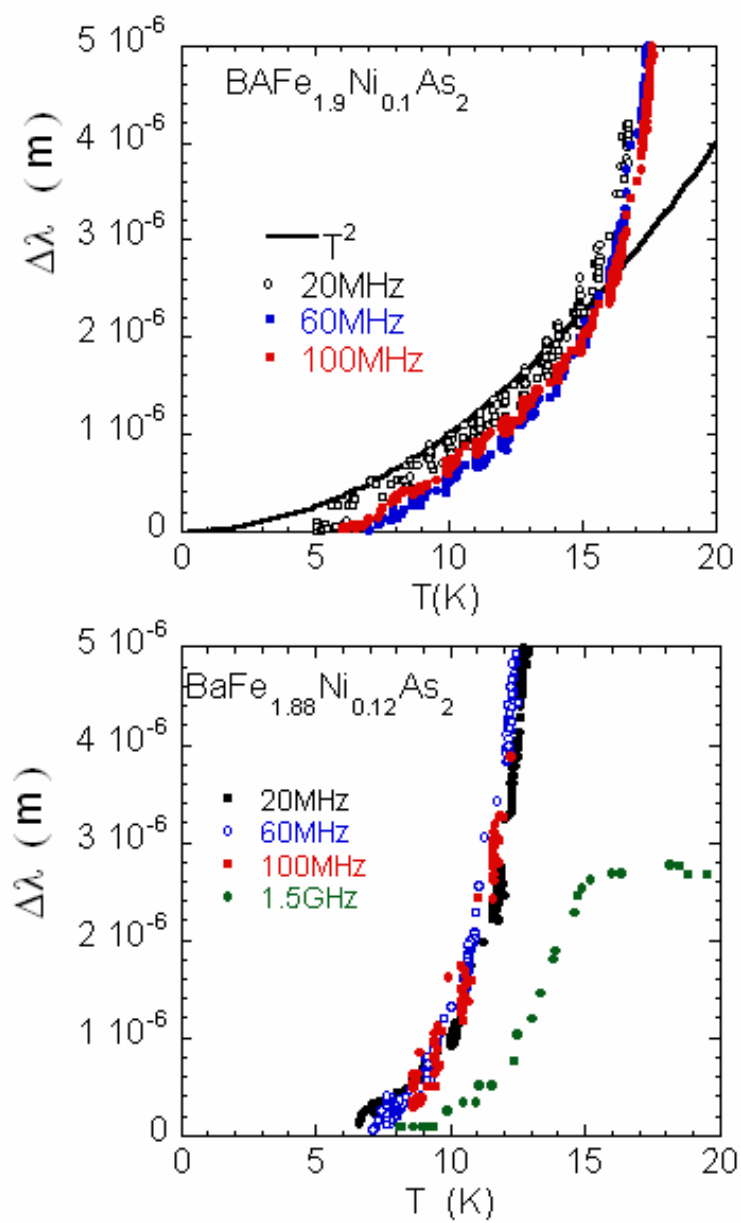


Fig3

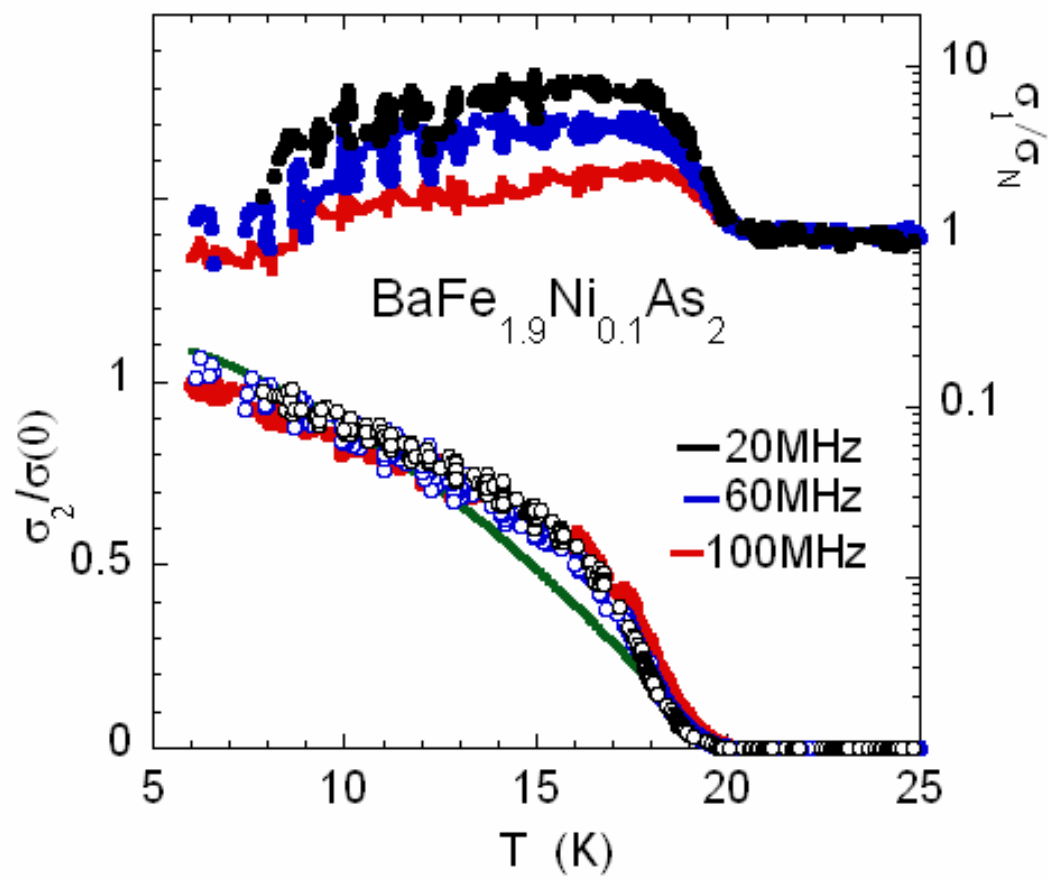


Fig4

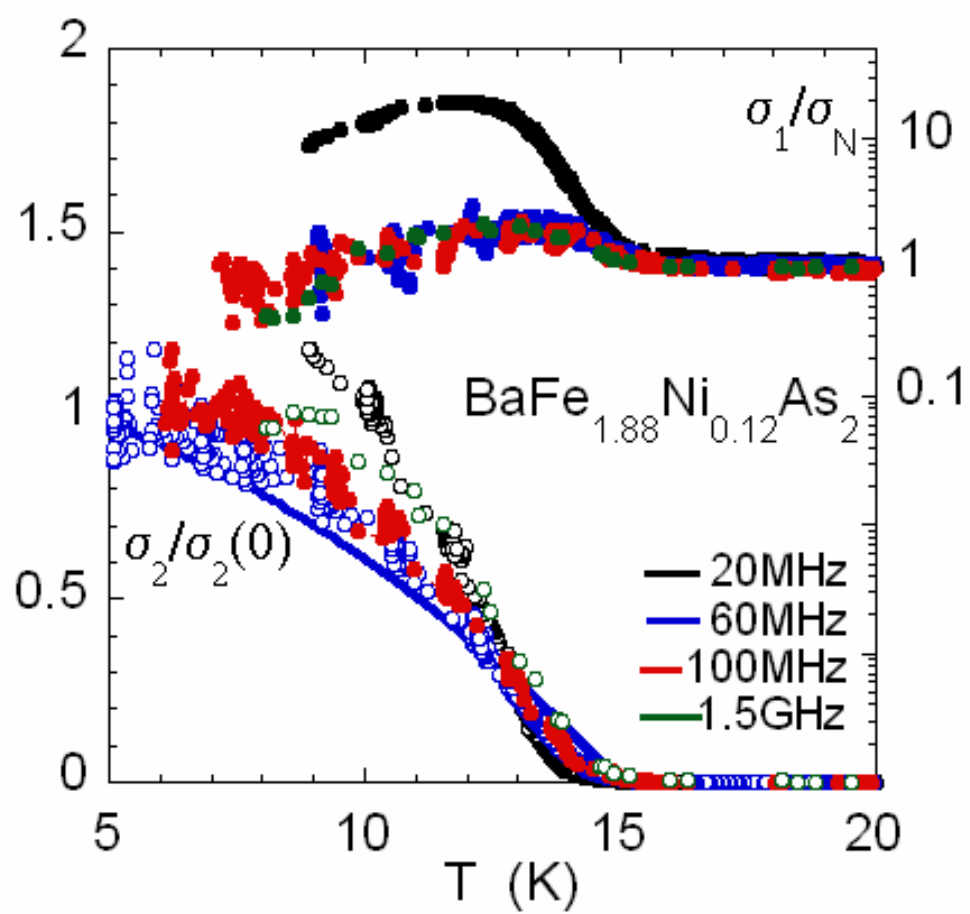


Fig5

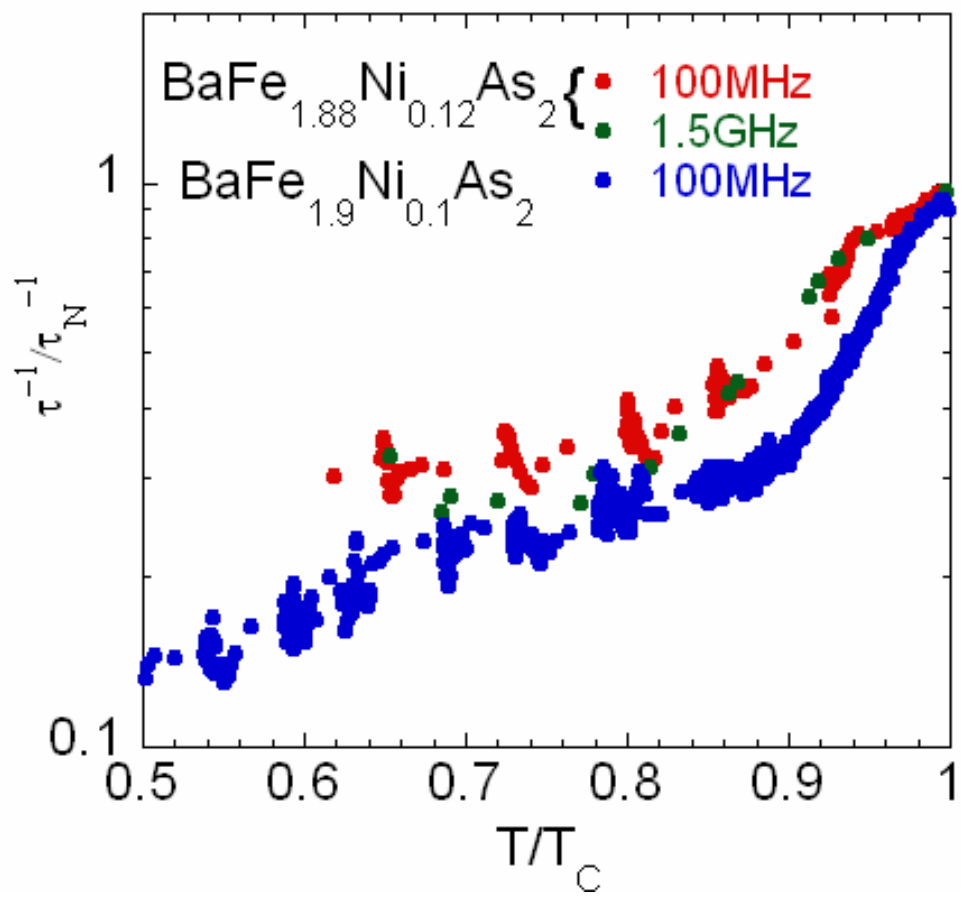


Fig6